

# Newtonian dynamics in the plane corresponding to straight and cyclic motions on the hyperelliptic curve $\mu^2 = \nu^n - 1$ , $n \in \mathbb{Z}$ : ergodicity, isochrony, periodicity and fractals

P. G. Grinevich<sup>1,a</sup> and P. M. Santini<sup>2,b</sup>.

<sup>1</sup> Landau Institute for Theoretical Physics, Moscow, Russia

<sup>2</sup> Dipartimento di Fisica, Università di Roma "La Sapienza" and  
Istituto Nazionale di Fisica Nucleare, Sezione di Roma

<sup>a</sup>pgg@itp.ac.ru

<sup>b</sup>paolo.santini@roma1.infn.it

## Abstract

We study the complexification of the one-dimensional Newtonian particle in a monomial potential. We discuss two classes of motions on the associated Riemann surface: the rectilinear and the cyclic motions, corresponding to two different classes of real and autonomous Newtonian dynamics in the plane. The rectilinear motion has been studied in a number of papers, while the cyclic motion is much less understood. For small data, the cyclic time trajectories lead to isochronous dynamics. For bigger data the situation is quite complicated; computer experiments show that, for sufficiently small degree of the monomial, the motion is generically periodic with integer period, which depends in a quite sensitive way on the initial data. If the degree of the monomial is sufficiently high, computer experiments show essentially chaotic behaviour. We suggest a possible theoretical explanation of these different behaviours. We also introduce a one-parameter family of 2-dimensional mappings, describing the motion of the center of the circle, as a convenient representation of the cyclic dynamics; we call such mapping the center map. Computer experiments for the center map show a typical multi-fractal behaviour with periodicity islands. Therefore the above complexification procedure generates dynamics amenable to analytic treatment and possessing a high degree of complexity.

# 1 From Newtonian systems to the motion on Riemann surfaces

In this paper we investigate the following two classes of autonomous Newtonian dynamical systems in the plane

$$\begin{aligned}\ddot{\mathbf{x}} &= \mathbf{F}_1^{(m)}(\mathbf{x}), \quad m \in \mathbb{Z}, \quad m \neq -1, \\ \ddot{\mathbf{x}} &= \mathbf{F}_2^{(m)}(\mathbf{x}, \dot{\mathbf{x}}), \quad m \in \mathbb{Z}, \quad m \neq -1,\end{aligned}\tag{1}$$

where  $\mathbf{x} = (x, y) \in \mathbb{R}^2$ , and  $\ddot{f} = d^2f/dt^2$ . The forces  $\mathbf{F}_{1,2}^{(m)}$  are defined by

$$\begin{aligned}\mathbf{F}_1^{(m)}(\mathbf{x}) &\equiv -(\operatorname{Re}(\alpha^2(x + iy)^m), \operatorname{Im}(\alpha^2(x + iy)^m)), \\ \mathbf{F}_2^{(m)}(\mathbf{x}, \dot{\mathbf{x}}) &\equiv -\dot{\mathbf{x}} \wedge \mathbf{h}_m - 8\pi^2 \frac{m+1}{(m-1)^2} \mathbf{x} - (\operatorname{Re}(x + iy)^m, \operatorname{Im}(x + iy)^m),\end{aligned}\tag{2}$$

where the constant vectors  $\mathbf{h}_m$ ,  $m \in \mathbb{Z}$  are orthogonal to the  $(x, y)$  plane, with  $\|\mathbf{h}_m\| = 2\pi \frac{m+3}{m-1}$ , and  $\alpha \in \mathbb{C}$  is an arbitrary parameter.

The classes (1a) and (1b) originate from the same complex ODE:

$$\frac{d^2\zeta}{d\tau^2} = -\zeta^m, \quad m \in \mathbb{Z}, \quad m \neq -1, \quad \tau \in \mathbb{C}, \quad \zeta \equiv \zeta(\tau) \in \mathbb{C},\tag{3}$$

solved by the complex quadrature

$$\begin{aligned}\tau &= \int_{\zeta(0)}^{\zeta} \frac{d\zeta}{\sqrt{2(E - \frac{\zeta^n}{n})}}, \\ E &= \frac{1}{2} \left( \frac{d\zeta}{d\tau}(0) \right)^2 + \frac{1}{n} (\zeta(0))^n, \quad n = m + 1.\end{aligned}\tag{4}$$

The first class (1a) is directly obtained from (3) via the following change of independent variables

$$\begin{aligned}z(t) &= x(t) + iy(t) = \zeta(\tau), \\ \tau(t) &= \alpha t, \quad \alpha \in \mathbb{C}\end{aligned}\tag{5}$$

corresponding to a rectilinear motion on the hyperelliptic curve of the quadrature (4); the second class (1b) is instead connected to (3) via the following change of dependent and independent variables (Calogero's transformation) [1]:

$$\begin{aligned}z(t) &= x(t) + iy(t) = \exp\left(\frac{i4\pi t}{n-2}\right) \zeta(\tau), \\ \tau(t) &= \frac{\exp(i2\pi t) - 1}{2\pi i}.\end{aligned}\tag{6}$$

Equation (6b) implies that, as the “physical time”  $t$  travels onward along the real  $t$ -axis, the motion of the complex time  $\tau$  is cyclic; the auxiliary transformation (6a) is what makes the Newtonian class (1b) autonomous.

Through the change of variables

$$\begin{aligned} w(\xi) &= c_1 \zeta(\tau), \quad \xi = c_2 \tau + \xi_0, \\ c_1 &= \left(\frac{1}{nE}\right)^{\frac{1}{n}}, \quad c_2 = \sqrt{2} (E)^{\frac{n-2}{2n}} \left(\frac{1}{n}\right)^{\frac{1}{n}}, \quad \xi_0 = \int_0^{c_1 \zeta(0)} \frac{dw}{\sqrt{1-w^n}}, \end{aligned} \quad (7)$$

the quadrature (4) takes its adimensional form. We have 2 cases, corresponding to  $n$  positive and  $n$  negative respectively:

$$\xi = \int_0^w \omega, \quad (8)$$

$$\omega = \frac{dw}{\sqrt{1-w^n}}, \quad n > 0; \quad \omega = \sqrt{\frac{w^{|n|}}{w^{|n|}-1}} dw, \quad n < 0. \quad (9)$$

Therefore the Newtonian systems (1a) and (1b) correspond, via (5), (6), (7), respectively to the rectilinear motion in the  $\xi$ -plane:

$$\xi = \xi_0 + \alpha c_2 t \quad (10)$$

and to the cyclic motion in the  $\xi$ -plane:

$$\begin{aligned} \xi &= \xi_c + R \exp(i(2\pi t + \varphi)), \\ \xi_c &= \xi_0 - \frac{c_2}{2\pi i}, \quad R = \frac{|c_2|}{2\pi}, \quad \varphi = \arg(-ic_2), \end{aligned} \quad (11)$$

where  $\xi_c$  and  $R$  are the center and the radius of the corresponding circle. We remark that the Cauchy data of the Newtonian dynamics (1b) determine completely this circle and the initial point on it.

To express  $w$  as a function of  $t$  we have to invert the hyperelliptic integrals (8), (9) defined on the surfaces

$$\Gamma : \mu^2 = 1 - w^{|n|}, \quad n > 0 \text{ or } n = 2k < 0, \quad (12)$$

$$\Gamma_1 : \mu^2 = w - w^{|n|+1}, \quad n = 2k + 1 < 0; \quad (13)$$

therefore the trivial dynamics (10) and (11) in the  $\xi$ -plane result in highly nontrivial motions on  $\Gamma, \Gamma_1$ .

Let us point out that, for  $n > 0$ , we have the problem of inverting a hyperelliptic integral defined by a **holomorphic** 1-form, and for  $n < 0$  we have to invert an integral defined by a **meromorphic** 1-form. As we shall see below, if the motion is rectilinear, the case  $n < 0$  is much simpler from the dynamical point of view.

The rectilinear motion on Riemann surfaces can be naturally interpreted as Hamiltonian system with a multivalued Hamiltonian ( or, equivalently, as a Hamiltonian system defined by a Hamiltonian 1-form with non-zero periods, see review [18]). This motion was intensively studied in the literature (references can be found in the reviews [24, 11]). A new description of the topology of these flows was suggested recently in [19].

The interest to this problem was partially motivated by its connections to stochastic dynamics. Consider a cycle on the Riemann surface transversal to the flow. The Poincaré map on this cycle preserves the measure on the cycle, therefore it can be interpreted as the interval exchange map, which is one of the basic stochastic models. Moreover, any interval exchange map can be obtained from this construction. It turns out that the properties of this map are deeply connected with the geometry of the moduli spaces [13, 17, 22, 24, 25, 26]. In particular, the Lyapunov exponents for this map at generic points can be calculated in terms of the Lyapunov exponents for the geodesic flow on the Teichmüller space.

Another motivation for the study of rectilinear motions comes from solid state physics: the conductivity tensor for metals in a “strong enough” magnetic fields is deeply connected to the quasiclassical electron motion on the Fermi-surface, which is a Hamiltonian flow on the Fermi-surface, and the Hamiltonian 1-form is determined by the direction of the magnetic field [16], [11]. In contrast to the case of the interval exchange map, the holomorphic form is now non-generic, and its real part has exactly 3 non-zero periods; therefore this situation needs a separate study.

The study of cyclic motions on Riemann surfaces was initiated in [1], where a general procedure, involving the change of variable (6), was introduced to deform large classes of ODEs so that they feature a lot of periodic solutions. The deformed dynamical systems are isochronous for initial data lying in a certain domain of full dimensionality (corresponding to the situation in which the circle is contained inside the analyticity disc of the unmodified ODE). Outside this domain, the circle may include branch points;

then bifurcations occur, and either the motion becomes periodic with multiple period, or the periodicity is lost and the system may exhibit sensitive dependence on the initial data (see [1, 2, 6, 9, 7, 3, 4, 8] and references therein quoted). This mathematical mechanism was first described in [9, 7]. As it was shown in [8] for an aristotelian 3-body problem which allows for a quite explicit analytical treatment, the transition from regular (periodic) to irregular (with sensitive dependence on the initial data) dynamics takes place when an infinity of branch points of the solution are arbitrarily close to the real  $t$ -axis.

A very general class of autonomous dynamical systems obtained through Calogero's transformation has been constructed in [5] (see also [15]). This class contains, in particular, systems of ODEs solved by quadratures associated with elliptic and hyperelliptic curves; the first investigation of some examples of this type was presented in [15]. Also the Newtonian systems (1b), corresponding to cyclic motions on the Riemann surface of the quadratures (4), are examples belonging to this general class. A detailed study, analytical and computational, of the systems (1b) in the particular cases  $n = 4, 5, 6$  has been recently done in [12], with the following results. In the elliptic case  $n = 4$  the motions are isochronous with period 1; if  $n = 6$  the hyperelliptic curve doubly covers an elliptic curve, and all motions are periodic with periods 1 or 2. In the more interesting case  $n = 5$ , numerical experiments seem to indicate that all solutions are periodic, with arbitrarily large period. The results contained in [5, 15, 12] have been the main motivation of our study.

**Remark 1.** The cyclic motion can be described as the motion with constant geodesic curvature on the Riemann surface with almost everywhere flat singular metric (or, equivalently, as the motion with a constant geodesic curvature on a polyhedron). As it was pointed out by S.P.Novikov [18], in the 2-dimensional case the motion with a prescribed geodesic curvature can be naturally interpreted as the Hamiltonian motion in magnetic field.

**Remark 2.** Under the change of variables (5), the complex Newtonian equation (3) becomes  $\ddot{z} = -\alpha^2 z^m$ , and can be cast into the complex Hamiltonian form:

$$\begin{aligned} \dot{z} &= \frac{\partial \mathcal{H}}{\partial \pi}, & \dot{\pi} &= -\frac{\partial \mathcal{H}}{\partial z}, & z, \pi &\in \mathbb{C}, \\ \mathcal{H}(z, \pi) &\equiv \frac{\pi^2}{2} + \frac{\alpha^2}{n} z^n, & \pi &= \dot{z}. \end{aligned} \tag{14}$$

Then it follows that also the corresponding dynamical systems (1a) can be

written in Hamiltonian form:

$$\begin{aligned} \dot{x} &= \frac{\partial H}{\partial p_x}, & \dot{y} &= \frac{\partial H}{\partial p_y}, \\ \dot{p}_x &= -\frac{\partial H}{\partial x}, & \dot{p}_y &= -\frac{\partial H}{\partial y}, \end{aligned} \tag{15}$$

where the canonically conjugated real variables  $\vec{x} = (x, y)$  and  $\vec{p} = (p_x, p_y)$  are defined by  $z = x + iy$ ,  $\pi = p_x - ip_y$ , and the Hamiltonian  $H(\vec{x}, \vec{p})$  is the real part of  $\mathcal{H}$  (the general procedure to go from complex to real Hamiltonian formulations can be found in [21]). In addition, the real and imaginary parts of  $\mathcal{H}$  are constants of motion in involution for the Hamiltonian system (15). Therefore the Newtonian equations (1a) are Liouville integrable, with polynomial (if  $n > 0$ ) or rational (if  $n < 0$ ) constants of motion in involution. But this Liouville integrability **is not global**. Indeed, a simple local analysis shows that the singularities of  $\vec{x}(t)$  and  $\vec{p}(t)$  in the complex  $t$ -plane are, for  $n \neq 3, 4$ , branchpoints (see (20)). In addition, for  $n \neq 6$ , such branch points are everywhere dense in the complex  $t$ -plane,  $\vec{x}$ ,  $\vec{p}$  are unbounded and the 2-dimensional real variety defined by the two constants of motion is not a torus (in particular, global action - angle variables cannot be defined). The existence of everywhere dense branch point singularities, which causes the lack of global integrability in the Liouville sense, turns out to be the reason for the sensitive dependence on the initial conditions exhibited by the corresponding dynamics, discussed in the following sections.

For the Newtonian class (1b), which clearly inherits from (3) and (6) the two  $t$ -dependent first integrals  $\tilde{H}$ ,  $\tilde{K}$ :

$$\begin{aligned} \tilde{H} &= \text{Re } \tilde{\mathcal{H}}, & \tilde{K} &= \text{Im } \tilde{\mathcal{H}}, \\ \tilde{\mathcal{H}} &\equiv \left[ \frac{1}{2} (\dot{z} - i \frac{4\pi}{n-2} z)^2 + \frac{z^n}{n} \right] e^{-i \frac{4\pi n}{n-2} t}, \end{aligned} \tag{16}$$

no Hamiltonian structure is instead known. Only after fixing the energy level, one obtains the Hamiltonian interpretation contained in the Remark 1.

**Remark 3.** The idea that the integrability or the non-integrability of a dynamical system be intimately related to the analyticity properties of its solutions in the complex time plane goes back to Jacobi, Kowalewski, Painlevé and other eminent mathematicians. For Kowalewski, Painlevé and his school, the request that the only movable singularities of ODEs be poles has been a very successful tool to isolate and classify important integrable cases [14]. The idea that integrability is compatible even with the presence of movable

branch point singularities, provided that they are not dense in the complex time plane, is more recent, and one of us (PMS) heard several illuminating lectures on this topic by Kruskal, more than 20 years ago. The works [23, 20] are some of the contributions connected to this fascinating idea.

As we shall see in the following sections, the Newtonian systems (1) are just distinguished examples of ODEs whose solutions exhibit branch point singularities which are everywhere dense in the complex time plane. Therefore the results presented in this paper can also be viewed as a contribution along this line of thinking.

The paper is organized as follows. In §2 we discuss the topological properties of the Riemann surfaces associated with the quadratures (8),(9), for a generic  $n \in \mathbb{Z}$ . In §3 we concentrate on the physically relevant subcase in which the degree  $n$  of the monomial is even, restricting further our analysis to a suitably factorized Riemann surface. In §4 we discuss the main properties of the rectilinear and cyclic motions on such factorized surfaces, as the degree  $n$  of the monomial varies. In §5 we associate with the cyclic motion the 1-parameter family of 2-dimensional mappings describing the dynamics of the center of the circle; such mappings show typical multi-fractal behavior with periodicity islands. In §6 we briefly comment on how the complexification procedures discussed in this paper can be a distinguished way of generating dynamics exhibiting a high degree of complexity and, at the same time, amenable in principle to analytical treatments.

## 2 Riemann surfaces associated with the Newtonian dynamics: generic case

In this section we introduce a description of the Riemann surfaces associated with the quadratures (8)-(9). This description is different from that used in [12].

$\mathbf{n} > \mathbf{0}$ . In the case  $n > 0$  we use the following representation for the surface  $\Gamma$ . Due to the rotation symmetry of  $\Gamma$ , it is convenient to draw the cuts in the  $w$ -plane as rays connecting the branch points (the  $n$  roots of unity) to infinity. Then we have 2 sheets and the map (8) maps each of them to a regular  $n$ -gone (see Fig 1):

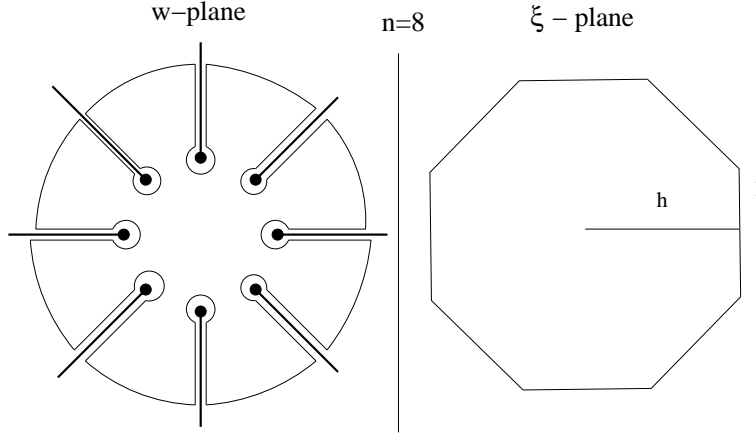


Fig 1.

Therefore the whole Riemann surface is represented by the union of 2 regular  $n$ -gons, and each side of the first  $n$ -gone is glued to the opposite side of the second one. Equivalently, we can attach one side of the first  $n$ -gone to the corresponding side of the second one. As the result of the above operation, we obtain a  $(2n-2)$ -gone, and  $\Gamma$  is obtained by gluing the opposite sides (see Fig 2).

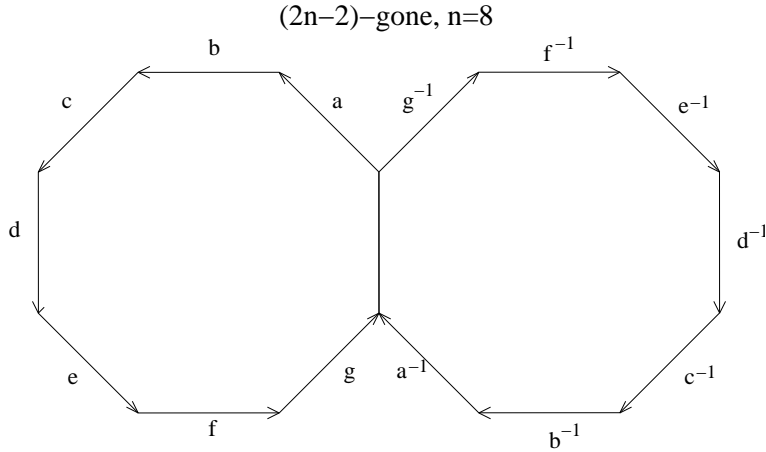


Fig 2.

Let  $g(\Gamma)$  be the genus of  $\Gamma$ ; then, for both  $n = 2k$  and  $n = 2k - 1$ ,  $g(\Gamma) = k - 1$ . The length of each side is equal to

$$l = 2 \int_1^{\infty} \frac{dw}{\sqrt{w^n - 1}} \quad (17)$$



and the distance  $h$  from the center to the sides satisfies the relation  $l = 2h \tan(\pi/n)$ .

If  $n$  is even, it is also convenient to define the factorized Riemann surface  $\tilde{\Gamma}$ , obtained by the factorization

$$w \rightarrow -w, \quad \mu \rightarrow -\mu. \quad (18)$$

$\tilde{\Gamma}$  can be naturally treated as the result of gluing the opposite sides of a single regular  $n$ -gone [10]. If  $n = 4k$  or  $n = 4k + 2$ , then  $g(\tilde{\Gamma}) = k$ .

**$n < 0$ .** In the case  $n < 0$  it is convenient to draw the cuts as rays connecting the roots of unity to 0. If  $n$  is even:  $n = 2k$ , we have 2 sheets and the map (9) maps each of them to the exterior (complement) of the regular  $|n|$ -gone. Therefore the whole Riemann surface  $\Gamma$  is represented by the union of the complements to 2 regular  $|n|$ -gons, and each side of the first  $|n|$ -gone is glued to the opposite side of the second one. Topologically, the exterior of an  $n$ -gone with the infinite point added is an  $n$ -gone; therefore  $\Gamma$  can be represented again as the result of gluing the opposite sides of a  $(2n - 2)$ -gone.

If  $n$  is odd:  $n = 2k + 1$ , we have one sheet and the map (9) maps it to the exterior of a regular  $(2|n|)$ -gone, which is drawn on the Riemann surface of the function  $\sqrt{w}$ . The points of a side in one sheet are glued to the corresponding points of the side in the second sheet.

**Cycles.** In our situation it is more convenient to use, instead of the canonical basis of cycles, a more symmetric one. Since  $\Gamma$  is obtained by gluing the opposite sides of a  $(2n - 2)$ -gone, let us choose the center of this  $(2n - 2)$ -gone as the starting point and denote by  $C_j$  the cycles connecting the sides  $s_j$  and  $s_{j+n-1}$ ,  $j = 1, \dots, n - 1$  (see Fig 3).

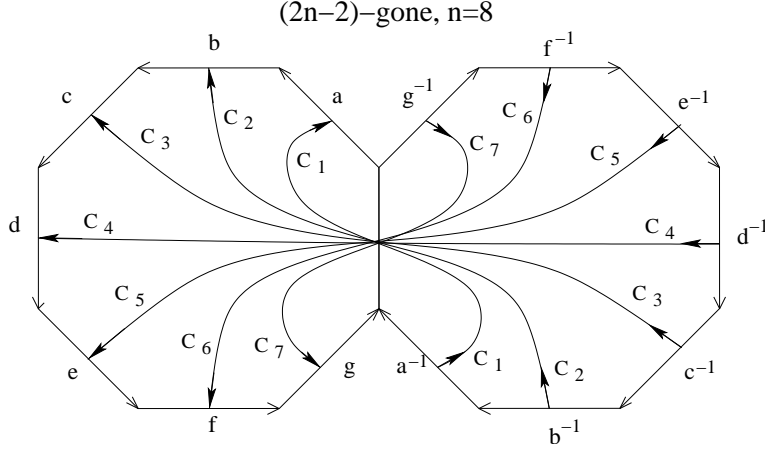


Fig 3.

If  $(n - 1)$  is even, these cycles are homologically independent,  $C_i \cdot C_j = 1$  for  $i < j$ . The fundamental group of  $\Gamma$  is generated by the  $C_j$  with the relation  $C_1 C_2^{-1} C_3 C_4^{-1} \dots C_{n-1}^{-1} C_1^{-1} C_2 C_3^{-1} C_4 \dots C_{n-1} = 1$ .

If  $(n - 1)$  is odd, these cycles are dependent. It is convenient to write the fundamental group of  $\Gamma$  as the group generated by  $C_j$ ,  $j = 1, \dots, k$  with two relations:  $C_1 C_2^{-1} C_3 C_4^{-1} \dots C_{n-1} = 1$ ,  $C_1^{-1} C_2 C_3^{-1} C_4 \dots C_{n-1}^{-1} = 1$ . In the homological group these two relations are equivalent and they imply that

$$C_1 - C_2 + C_3 - C_4 \dots + C_{n-1} = 0. \quad (19)$$

As usual, the multivaluedness of  $\xi(w)$ , associated with the above cycles, implies that the inverse function  $w(\xi)$  be multiperiodic. Moreover, the vertices of the  $n$ -gone are the only singularities of  $w(\xi)$ . If  $n = 3, 4$ , this singularities are poles and  $w(\xi)$  is single-valued. Otherwise, they are branch points  $\xi_b$ , and  $w(\xi)$  is unbounded near them. For  $n > 0$

$$w \sim c(\xi - \xi_b)^{-\frac{2}{n-2}}, \quad \xi \sim \xi_b. \quad (20)$$

Due to the above multiperiodicity, these singularities are everywhere dense in the complex plane for  $n \neq 3, 4, 6$ . These exceptional cases correspond to the equilateral triangle, the square and the regular hexagon, which are well-known to cover exactly the plane through the Schwarz reflection principle.

**Coverings.** The inversion of the hyperelliptic integrals leads us to the study of the motion not only on the surface  $\Gamma$ , but also on a proper covering space

$\hat{\Gamma}$ . It is well-known that there is a one-to-one correspondence between the subgroups  $\tilde{\pi}$  of the fundamental group  $\pi(\Gamma, x_0)$  and the non-ramified coverings of  $\Gamma$ . Namely, the paths  $\gamma \in \tilde{\pi}$  are exactly the loops which remain closed after being lifted to covering space. If  $\tilde{\pi}$  is the unit subgroup, we obtain the universal covering, which for  $g \geq 2$  is isometric to the Lobachevsky plane. But, for the problem of inverting the hyperelliptic integrals, it is much more natural to use “smaller” coverings:

1. The maximal Abelian covering (see [19]):  $\tilde{\pi}$  is the commutant of  $\pi$ , i.e. the subgroup generated by all elements of the type  $g_1 g_2 g_1^{-1} g_2^{-1}$ ,  $g_1, g_2 \in \pi(\Gamma, x_0)$ . A closed path in  $\Gamma$  remains closed in the covering space iff the integrals of all holomorphic forms (as well as the integrals of all meromorphic forms with only zero residues) along this path are equal to 0.
2. The covering  $\hat{\Gamma}$  associated with a given holomorphic form  $\omega$ : the subgroup  $\tilde{\pi}$  is formed by all closed paths  $\gamma$  such that

$$\oint_{\gamma} \omega = 0.$$

If all periods of  $\omega$  are linearly independent over the rational numbers, the covering defined by  $\omega$  coincides with the maximal Abelian one. But, if there is some rational dependence between the periods, it is smaller.

### 3 Riemann surfaces associated with the Newtonian dynamics: $n$ even

For simplicity, in the rest of the paper we concentrate only on the case of even  $n$ :  $n = 2k$ . We shall also impose the restriction  $n > 0$ . The reason is that for  $n < 0$  the rectilinear motion is trivial (see below), while the cyclic motion can be obtained from the case  $n > 0$  by time-reversal.

It is convenient to focus our attention on the motion on the factorized Riemann surface  $\tilde{\Gamma}$ . If the motion on  $\tilde{\Gamma}$  is periodic, then the motion on  $\Gamma$  is also periodic, and the two periods either coincide or the period on  $\Gamma$  is twice bigger, depending on whether the number of intersections with the sides is even or odd. Therefore the motion on  $\tilde{\Gamma}$  contains all the essential informations. The corresponding cycles are drawn in Fig 4.

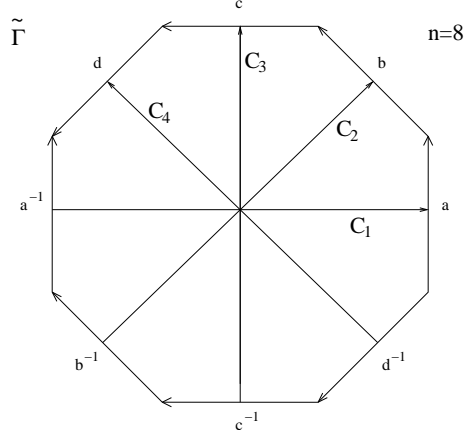


Fig 4.

Since our experiments cover the polygons with even  $n$ , from  $n = 8$  to  $n = 16$ , let us discuss the main properties of the corresponding Riemann surfaces  $\Gamma, \tilde{\Gamma}$ .

If  $n = 4$ ,  $\Gamma$  and  $\tilde{\Gamma}$  are tori:  $g(\Gamma) = g(\tilde{\Gamma}) = 1$ , and the universal covering coincides with the maximal Abelian covering and is exactly the complex plane. The basic periods are  $2h$  and  $2ih$ , and they are independent.

If  $n = 6$ ,  $\tilde{\Gamma}$  is again a torus,  $g(\tilde{\Gamma}) = 1$ ,  $g(\Gamma) = 2$ , and  $\Gamma$  is a ramified covering of  $\tilde{\Gamma}$  with 2 branch points. The periods along the cycles  $C_1, C_2, C_3$  are  $2h, 2e^{i\pi/3}h, 2e^{2i\pi/3}h$  respectively, and their alternated sum is equal to 0. Let us recall that, homologically,  $C_1 - C_2 + C_3 = 0$ . The covering  $\hat{\Gamma}$  corresponding to our integral coincides with the maximal Abelian covering.

If  $n = 8$ ,  $g(\tilde{\Gamma}) = 2$ ,  $g(\Gamma) = 3$  and  $\Gamma$  is a non-ramified covering of  $\tilde{\Gamma}$ . The basic periods of  $\tilde{\Gamma}$  are  $2h, 2e^{i\pi/4}h, 2e^{i\pi/2}h, 2e^{3i\pi/4}h$ , and they are independent over the rational numbers. Therefore the covering  $\hat{\Gamma}$  associated with our integral again coincides with the maximal Abelian covering.

If  $n = 10$ ,  $g(\tilde{\Gamma}) = 2$ ,  $g(\Gamma) = 4$  and  $\Gamma$  is a ramified covering of  $\tilde{\Gamma}$  with 2 branch points. The basic periods of  $\tilde{\Gamma}$  are  $2h, 2e^{i\pi/5}h, 2e^{2i\pi/5}h, 2e^{3\pi/5}h, 2e^{4i\pi/5}h$ , and the basic relation is  $C_1 - C_2 + C_3 - C_5 + C_5 = 0$ . Again the covering  $\hat{\Gamma}$  associated with our integral coincides with the maximal Abelian covering.

If  $n = 12$ ,  $g(\tilde{\Gamma}) = 3$ ,  $g(\Gamma) = 5$  and  $\Gamma$  is a non-ramified covering of  $\tilde{\Gamma}$ . The basic periods of  $\tilde{\Gamma}$  are  $2h, 2e^{i\pi/6}h, 2e^{i\pi/3}h, 2e^{i\pi/2}h, 2e^{2i\pi/3}h, 2e^{5i\pi/6}h$ ; therefore

$$\oint_{C_1 - C_3 + C_5} \omega = \oint_{C_2 - C_4 + C_6} \omega = 0. \quad (21)$$

It is the first case in which we have nontrivial integer relations between the periods: we have 6 independent directions in the universal covering, but only 4 of them remain independent on the covering  $\hat{\Gamma}$  associated with our hyperelliptic integral.

If  $n = 14$ ,  $g(\tilde{\Gamma}) = 3$ ,  $g(\Gamma) = 6$  and  $\Gamma$  is a ramified covering of  $\tilde{\Gamma}$  with 2 branch points. The only relation between the periods is the one prescribed by the homological group:  $C_1 - C_2 + C_3 - C_4 + C_5 = 0$ . The covering  $\hat{\Gamma}$  associated with our integral coincides with the maximal Abelian covering.

The last case studied in our numerical experiments is  $n = 16$ . In this case  $g(\tilde{\Gamma}) = 4$ ,  $g(\Gamma) = 7$  and  $\Gamma$  is a non-ramified covering of  $\tilde{\Gamma}$ . The basic periods of  $\tilde{\Gamma}$  are independent over the rational numbers, and we have the full Abel covering.

The points of the maximal Abelian covering are represented by the points of the basic polygon plus the total shift

$$\mathcal{T} = \sum_{j=1}^k m_j C_j, \quad (22)$$

where  $m_j$  is the number of crossings of the trajectory with the side  $s_j$  minus the number of crossings with the opposite side  $s_{j+k}$ . For odd  $k$ , the relation (19) should be taken into account. The simplest way is to substitute  $C_k = -C_1 + C_2 + \dots + C_{k-1}$  into (22), obtaining

$$\mathcal{T} = \sum_{j=1}^{k-1} (m_j + (-1)^j m_k) C_j. \quad (23)$$

Due to the rotation symmetry of  $\tilde{\Gamma}$ , we can have extra integer relations among the periods of the form. For instance, if  $n = 4lk'$ , where  $l$  is odd, the cycles  $C_m, C_{m+2k'}, C_{m+4k'}, \dots, C_{m+2k'(l-1)}$  are independent, but the corresponding periods satisfy the relations:

$$\oint_{C_m - C_{m+2k'} + C_{m+4k'} + \dots + C_{m+2k'(l-1)}} \omega = 0, \quad m = 1, 2, \dots, 2k'; \quad (24)$$

see, for instance, (21) for  $n = 12$ . In these cases, instead of studying the maximal Abelian covering, we study the smaller covering  $\hat{\Gamma}$  associated with our hyperelliptic integral, and we have extra relations. Therefore

$$\mathcal{T} = \sum_{j=1}^{\tilde{n}} \tilde{m}_j C_j \quad (25)$$

for suitable  $\tilde{m}_j$ , where  $\tilde{n}$  is the number of independent periods.

## 4 Rectilinear and cyclic motions

**Rectilinear motion.** If  $n < 0$  the qualitative picture is rather simple. The integrand is a meromorphic differential, and each trajectory goes to  $\infty$  for  $t \rightarrow \pm\infty$ . In terms of the vector field, it means that we have either 2 (for even  $n$ ) or 1 (for odd  $n$ ) fixed points, all the trajectories reach them in an infinite time, and generic initial conditions result in regular motions without sensitive dependence on the initial condition.

If  $n > 0$  we are in the situation in which the Hamiltonian flow is defined by a holomorphic form. The basic features of such motion for  $g > 1$  were intensively studied by many authors (see the literature at the end of §1). It is convenient to choose a Poincaré cycle transversal to the flow, and study the corresponding Poincaré map. For a given trajectory, the number  $N$  of intersections with the Poincaré cycle is used as the discrete time.

For generic data (a generic algebraic Riemann surface and a generic holomorphic form) the motion is aperiodic, the image on the maximal Abelian covering has a distinguished direction  $\vec{v}_0$  (which is Poincaré dual to the cohomological class of the form). In our case

$$\vec{v}_0 = \sum_{j=1}^k (v_0)_j C_j \quad (26)$$

where

$$(v_0)_j = (\vec{\alpha}, \hat{n}_j), \quad \vec{\alpha} = (\operatorname{Re} \alpha, \operatorname{Im} \alpha), \quad \hat{n}_j = (\cos(2\pi(j-1)/n), \sin(2\pi(j-1)/n)), \quad (27)$$

$\hat{n}_j$  denotes the normal vector to the side  $s_j$ . Let us recall that, if  $n = 2k$  and  $k$  is odd, the vectors  $C_j$  are dependent, and for the maximal Abelian covering we can use the basis  $C_1, \dots, C_{k-1}$ . Then

$$\vec{v}_0 = \sum_{j=1}^{k-1} (\tilde{v}_0)_j C_j, \quad (\tilde{v}_0)_j = (v_0)_j + (-1)^j (v_0)_k. \quad (28)$$

If the number  $N$  of iterations is sufficiently large, the total shift from the starting point is described by the formula

$$\mathcal{T} = Nc\vec{v}_0 + o(N), \quad (29)$$

where  $c$  is an order 1 constant. The Poincaré map is ergodic, and this implies that, for any pair of arbitrary close initial points, the stripe between their trajectories sooner or later meets a branch point, located at the vertex of the polygon. After this event the trajectories separate to a distance of order 1. The difference between these trajectories is encoded in the  $o(N)$  term of the asymptotics. The corrections to the leading asymptotic term were studied in [25], [26] (see also the review [24]), where the following statements were proved:

1. Let us consider the projection  $P_{\vec{v}_0}$  along the vector  $\vec{v}_0$  to the complementary space. Then there exists a vector  $\vec{v}_1$  in this complementary space such that the projection has the form:

$$P_{\vec{v}_0}\mathcal{T} = N^{\lambda_1}c_1(N)\vec{v}_1 + o(N^{\lambda_1}), \quad 0 < \lambda_1 < 1. \quad (30)$$

where  $c_1(N)$  is a random function of  $N$  of order 1

2. For any given starting point, it is possible to define a special subsequence  $\{N_l\}$  such that, going from  $N_l$  to  $N_{l+1}$ , the trajectory returns much closer to the starting point (for details see [24]). Using this subsequence, it is possible to continue the above procedure, defining the vectors  $\vec{v}_2, \dots, \vec{v}_{g-1}$  and the sequence  $\lambda_2, \dots, \lambda_{g-1}$  such that  $1 > \lambda_1 > \lambda_2 \dots \lambda_{g-1} > 0$ .
3. If  $\circ$  denotes the intersection form on cycles, it generates a symplectic scalar product on vectors. In this symplectic product  $\vec{v}_i \circ \vec{v}_j = 0$  for all  $i, j$ .

If we consider a pair of close trajectories, after a sufficiently large number of iterations they deviate on the maximal Abelian covering, and, according to the formula (30), the distance on the maximal Abelian covering increases as  $N^{\lambda_1}$ . Therefore  $\lambda_1$  can be interpreted as the main Lyapunov exponent, and the remaining  $\lambda_j$ 's can be interpreted as the other Lyapunov exponents (see [24]). Additional information about the numerical values of these exponents for small  $g$  as well as some analytic results can be found in the review [24].

Formally, the results of the papers [24]-[26] are valid for generic Riemann surfaces, while our polygon is highly symmetric. But numerical experiments show good agreement with this theory.

**Cyclic motion.** As far as we know, the study of cyclic motions on Riemann surfaces began only recently (see the literature at the end of §1) and the picture is much less clear. Here we present the results of numerical experiments proceeded by the authors, and we give some preliminary qualitative explanation of the observed phenomena, based on the topological structure of the surface.

We always assume that our trajectories are generic in the following sense: they never hit the vertices of the polygon, otherwise the motion becomes undefined.

For the numerical simulations we used the following technique. As it was mentioned above, we make our calculations on  $\tilde{\Gamma}$ , which is represented by gluing the sides of the regular  $n$ -gone,  $n = 2k$ . In fact, to recover the dynamics on  $\Gamma$  for even  $n$ , it is sufficient to study the dynamics on  $\tilde{\Gamma}$  and check at each step if the number of intersections of our trajectory with the sides of the polygon is even or odd. If it is even, the trajectory is on the same sheet, and if it is odd, the trajectory is on the opposite sheet.

Any time our trajectory crosses the side of the polygon, it is shifted of the corresponding period.

In the cyclic case the trajectory is periodic iff, at some iteration, the total shift on the covering associated with the quadrature becomes zero.

We first discuss the exceptional cases. If  $n = 4$ ,  $\Gamma$  and  $\tilde{\Gamma}$  are tori,  $w(\xi)$  is single-valued and the motion is always periodic with period 1; i.e. it is isochronous. If  $n = 6$ ,  $\Gamma$  is a two-sheeted ramified covering of the torus  $\tilde{\Gamma}$  with two branch points. Therefore the motion is always periodic, with period 1 or 2, depending on whether the number of square root type branch points inside the trajectory is even or odd. These two cases have been already considered in [12].

We now discuss the non-exceptional cases.

For given  $n = 2k$ , if the diameter  $D$  of the circle is smaller than  $l$ , where  $l$  is the side length, the motion is periodic, and there is at most 1 branch point inside the circle. If there is no branch point inside, the period is 1 and the motion is isochronous; otherwise it is equal to  $(n - 2)/2$  for even  $k$  and to  $(n - 2)/4$  for odd  $k$ .

For bigger cycles the situation becomes much more complicated, and we studied it using a series of computer experiments, which have not exhausted the whole phase space. These experiments show the following.

1. The period is very sensitive to the radius  $R$  and to the position  $\xi_c$  of



the center of the circle.

2. Our observation shows an essential difference between the cases  $n = 8, 10, 12$  and  $n = 14, 16$ .

Let us discuss the first group  $n = 8, 10, 12$ . From the numerical experiments it seems that, for data of full measure, the motion is periodic, and the typical periods grow exponentially with the ratio  $D/l$ . We have observed periods of order  $10^8$  for  $D/l \sim 20$ . For bigger  $D$ , we have observed starting points for which the period was not found after  $2 \cdot 10^9$  iterations.

For  $n = 14$  and  $n = 16$  we have found that, for many initial configurations starting from  $D/l \sim 2$ , the period was not found after  $2 \cdot 10^9$  iterations. Our conjecture is that, in this cases, the aperiodic trajectories are non-exceptional.

3. If we consider the trajectories for which the period was either not found or was sufficiently large, the total shift on the covering space seems to exhibit the following behaviour:

$$\mathcal{T} \sim N^\lambda \vec{v}(N), \quad \lambda \sim \frac{1}{2}, \quad (31)$$

where  $N$  is the large number of iterations and  $\vec{v}(N)$  is a random vector of order 1. Therefore, the distance on  $\hat{\Gamma}$  of two close trajectories increases approximately as  $N^\lambda$ , and  $\lambda \sim \frac{1}{2}$  can be interpreted as the principal Lyapunov exponent.

Formula (31) suggests that, for sufficiently large  $N$ , the shift  $\mathcal{T}$  can be approximated by the random motion on a lattice. Now we show that, accepting this assumption, one can explain the difference between the above two classes.

Let us stress that, for cyclic motions, the total shift in the covering space can be arbitrarily large but, after being projected to the time-plane, the total shift is bounded by the condition:

$$\left| \sum_{j=1}^k m_j e^{(j-1)\pi/k} \right| < \frac{D}{2h} + 1/\cos(\pi/n). \quad (32)$$

This inequality imposes a severe constraint on the vector  $(m_1, \dots, m_k)$ . Let us denote by “effective dimension” the maximal number of  $m_j$ ’s which

can be chosen arbitrarily. If these components are fixed, there is only a finite number of options for the other components.

Let us point out that the effective dimension is equal to the number of independent shifts in the covering  $\hat{\Gamma}$  associated with the quadrature minus 2. Indeed, if we fix any pair of basic shifts, say  $e^{(j-1)\pi/k}$ ,  $j = 1, 2$ , which form a basis in the complex plane over  $\mathbb{R}$ , and we assign arbitrary integer values to all the other  $m_j$ 's ( $j \neq 1, 2$ ), then the two coefficients  $m_1, m_2$  are constrained by the inequality (32) to take only a finite number of values.

From the considerations made in Section 3, it follows that, for  $n = 8, 10, 12$  the effective dimension is 2, while for  $n = 14$  it is equal to 4 and for  $n = 16$  it is equal to 6.

On the basis of the numerical experiments we assume that, for sufficiently large  $N$ , our dynamics be approximated by a random motion in the “lattice of effective dimension”. It is well-known that, for the 2-d symmetric random motion, the probability to return to the starting point is equal to 1; therefore we expect that, with probability 1, this motion be periodic. If the dimension is higher than 2, with non-zero probability we do not return to the starting point, and there are aperiodic trajectories. Therefore the random hypothesis implies that, for  $n = 8, 10, 12$  (cases in which the effective dimension is 2) the typical motion is periodic, while for  $n = 14$  and  $n = 16$  (cases in which the effective dimension is greater than 2) there are aperiodic domains of positive measure, in agreement with our observations.

## 5 The center map as a fractal

In the rectilinear motion it is convenient to represent the dynamics on the surface in terms of the Poincaré map on a transversal cycle. It is the well-known “interval exchange map”. In the cyclic motion it is convenient to study the dynamics of the center  $\xi_c$  of the cycle, for any fixed radius  $R$ .

The dynamical rule is the following: any time the circle crosses a side  $s_j$  of the  $n$ -gone, the center is shifted in the following way:

$$\xi_c \rightarrow \xi_c - 2he^{2\pi(j-1)/n}. \quad (33)$$

It is a 1-parameter family of deterministic 2-dimensional mappings (the arbitrary parameter being the radius of the circle). We call this mapping the “center map”.

It is interesting to study the center map for aperiodic trajectories (of course, up to the computer experiment limits). Considering as basic illustrative example the polygon  $n = 16$ ,  $h = 1$  centered at the origin, we have made a series of experiments showing interesting generic multi-fractal behaviour with periodicity islands.

In the first set of experiments we fixed  $R = 0.358$  and we varied the initial position of the center. In Fig 5 we choose  $\xi_c = (1.1610, -0.4037)$ , obtaining the following fractal:

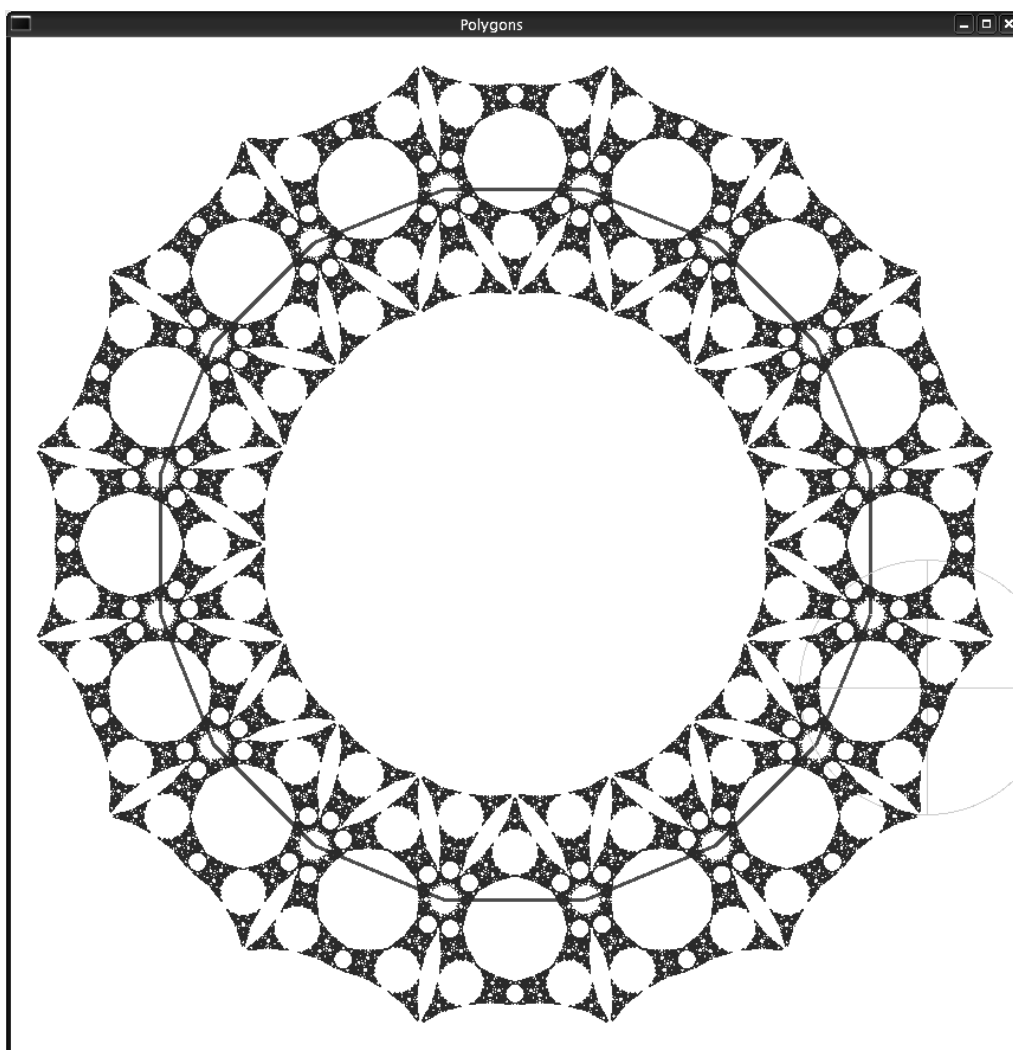


Fig 5.

In this figure, together with the fractal, we see also the 16-gone and the initial circle, located in the south-east position (it is drawn by a very thin line). The initial center  $\xi_c$  is marked by the intersection of the inner lines. We remark that this fractal shows the rotation symmetry of the polygone.

In Fig 6 we see the same fractal, but magnified 33 times. The initial center is marked again by the intersections of the inner lines.

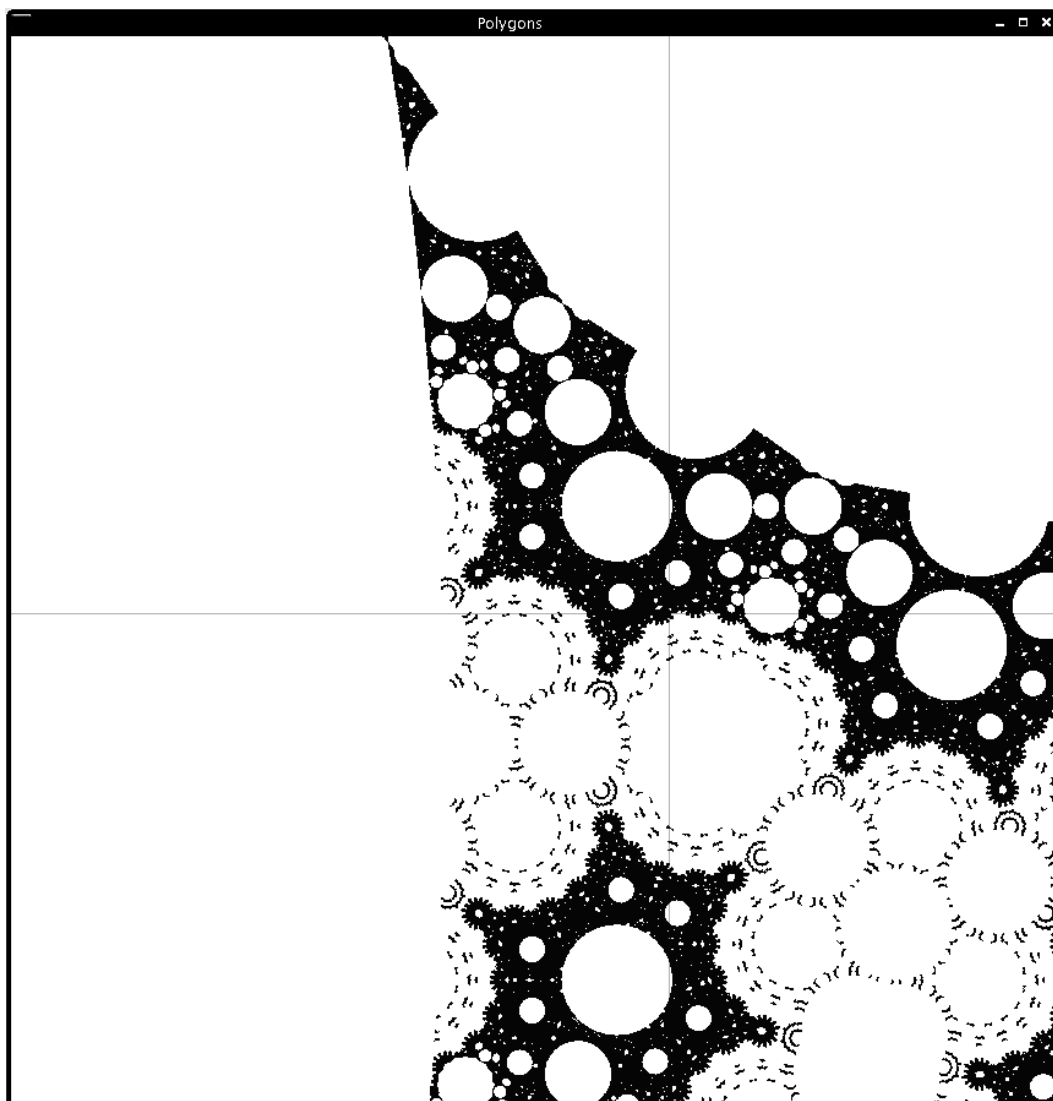


Fig 6.

This figure makes clear the fractal structure. It turns out that this fractal is the boundary of some islands inside which the center map is periodic with fixed periods. Typically the period increases as the size of the island decreases.

Choosing the starting point  $\xi_c$  inside the fractal region, we obtain a fractal coinciding with this one up to the picture resolution. Choosing the starting point  $\xi_c = (1.1572, -0.4151)$  outside the fractal, but on the boundary of the periodicity islands, we obtain a different fractal, living in the complementary region (see Fig 7).

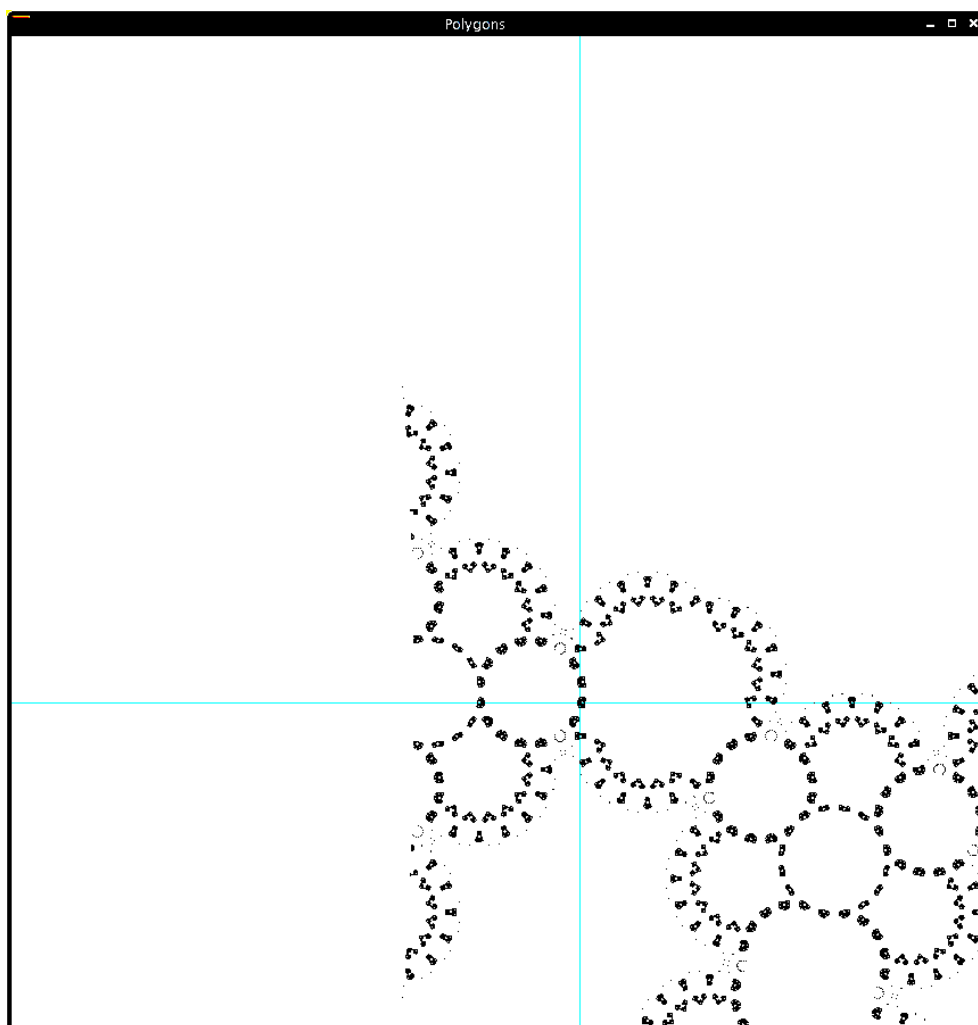


Fig 7.

In the second series of experiments we change the radius  $R$ . For a sufficiently small change of radius the fractal changes, but keeping all the principal features. Choosing, instead, a sufficiently different radius, we obtain completely different fractal pictures. For instance, for  $R = 0.6$ , we obtain the rich fractal shown in Fig 8 (compare it with the fractal in Fig 5).

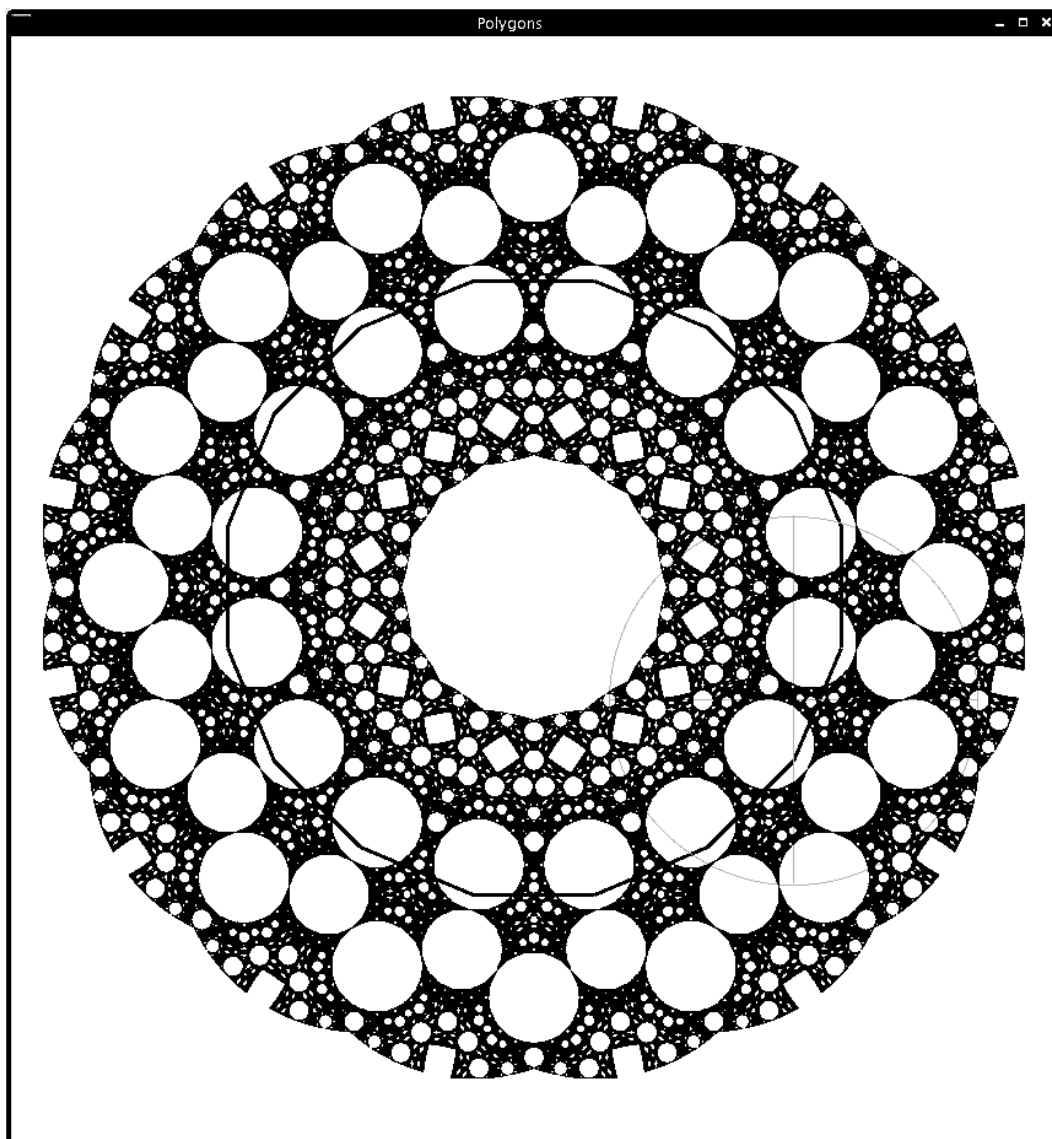


Fig 8.

Fig 9 shows a detail of the fractal of Fig 8, magnified 10 times, containing a part of the initial circle.

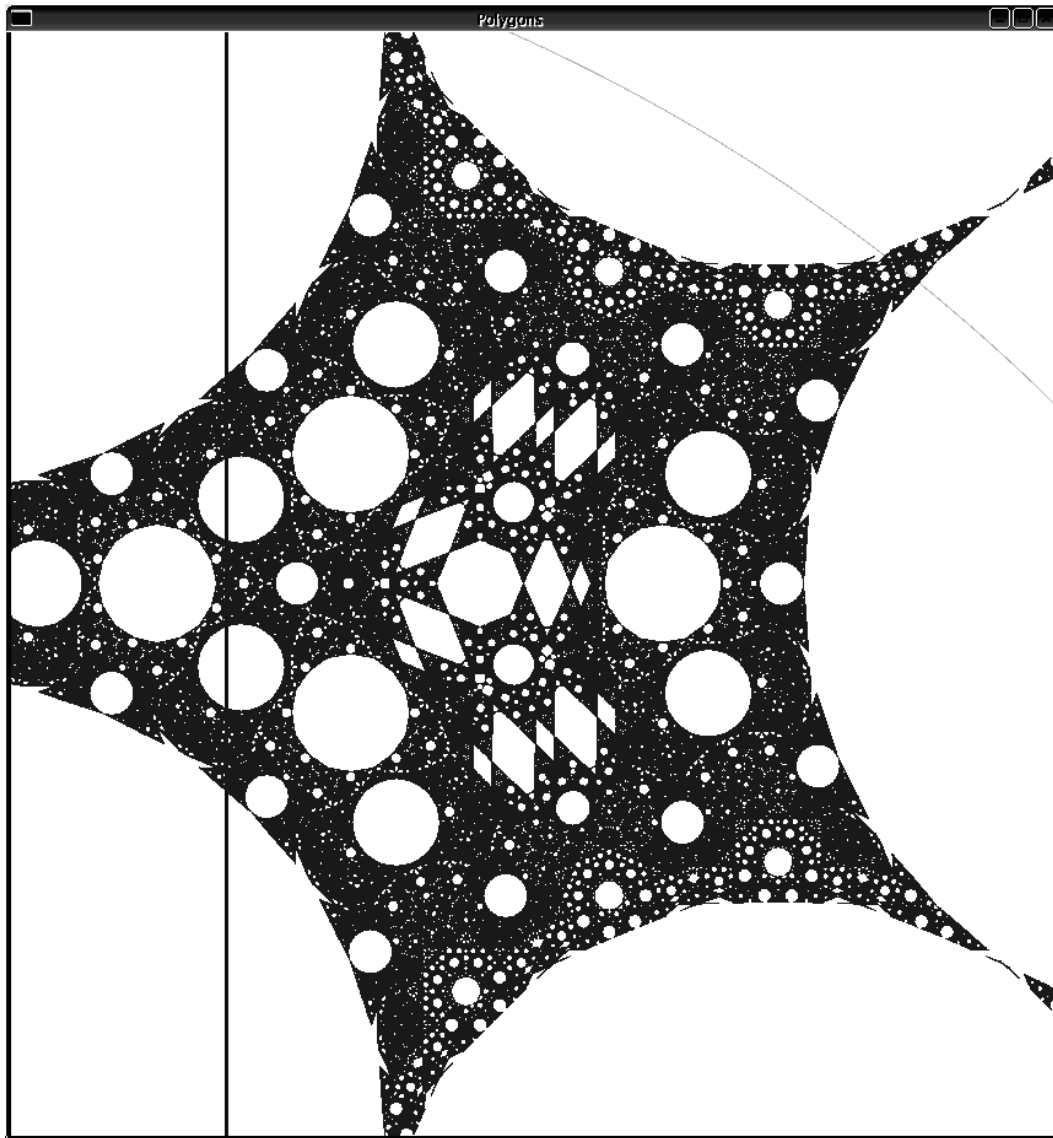


Fig 9.

Fig 10 shows a detail of Fig 9, magnified 4 times more. These magnifications make evident the extremely rich fractal nature of the center map.

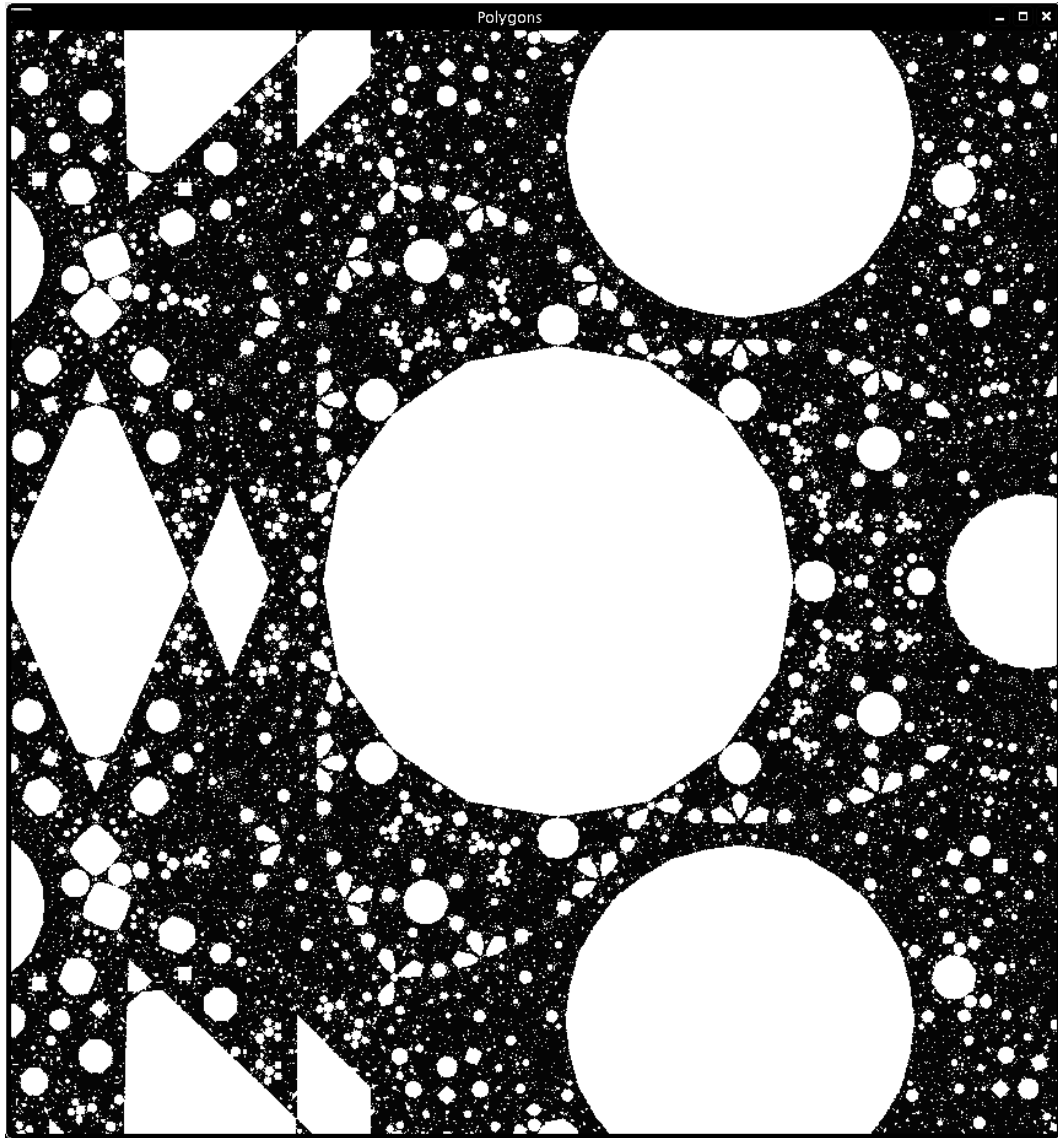


Fig 10.



## 6 Complexification and Complexity

We end this work with a consideration. The results of this paper strongly suggest that proper complexifications of dependent and independent variables of a given ODE are very fruitful and rich operations, enabling one to generate complicated dynamics amenable to exact analytical treatments. Indeed they allow to go, for instance, from the elementary one dimensional Newtonian motion in a monomial potential, to the complicated dynamics (1b), whose high degree of complexity is well illustrated by the fractal behavior of the associated center map (see §5). We feel that dynamics generated through complexification procedures could serve as prototypical examples of a new paradigm of chaos, potentially interesting in applications.

### Acknowledgements.

This research was initiated in collaboration with F. Calogero, who is also the initiator of the studies of dynamical systems associated with cyclic motions on Riemann surfaces. Unfortunately other duties prevented him from taking an active part in the development of the results reported in this paper, and he therefore preferred not to sign this paper, although he did participate in the very early stage of this research and he constantly encouraged our investigations. It is therefore a pleasure to us to acknowledge his important contribution, with the hope that he will join us in the future developments of this research.

PMS acknowledges useful discussions with D. Gomez-Ullate and Y. Fedorov concerning their results [12] on the analytical study of the dynamical systems (1b). These results, together with the results [5, 15] of F. Calogero and E. Induti, have been the main motivation for the present study. He also acknowledges the stimulating questions and remarks of the students of the specialistic course “Nonlinear evolutionary systems” he gave in the University of Roma “La Sapienza” in the Spring 2006, in which some of the ideas and results contained in this paper were first presented and tested.

The visit of PG to Rome was supported by the INFN grant 2006. PG was also supported by the RFBR grant 04-01-00403a.

## References

- [1] F. Calogero, “A class of integrable hamiltonian systems whose solutions are (perhaps) all periodic”, *J. Math. Phys.* **38** (1997), 5711-5719.
- [2] F. Calogero, *Classical Many-Body Problems Amenable to Exact Treatment*, Lecture Notes in Physics Monograph **m 66**, Springer, Berlin, 2001.
- [3] F. Calogero, “Partially superintegrable (indeed isochronous) systems are not rare”, in: *New trends in Integrability and Partial Solvability*, edited by A. B. Shabat, A. Gonzalez-Lopez, M. Manas, L. Martinez Alonso and M. A. Rodriguez, NATO Science Series, II. Mathematics, Physics and Chemistry, vol. **132**, Proceedings of the NATO Advanced Research Workshop held in Cadiz, Spain, 2-6 June 2002, Kluwer, 2004, pp. 49-77.
- [4] F. Calogero, “Periodic solutions of a system of complex ODEs”, *Phys. Lett. A* **293** 2002, 146-150.
- [5] F. Calogero, “Isochronous dynamical systems”, *Applicable Anal.* 85, 5-22 (2006).
- [6] F. Calogero and J. P. Francoise, “Periodic motions galore: how to modify nonlinear evolution equations so that they feature a lot of periodic solutions”, *J. Nonlin. Math. Phys.* **9** (2002), 99-125.
- [7] F. Calogero, J. P. Francoise and M. Sommacal, “Periodic solutions of a many-rotator problem in the plane. II. Analysis of various motions”, *J. Nonlinear Math. Phys.* **10**, 157-214 (2003).
- [8] F. Calogero, D. Gomez-Ullate, P. M. Santini and M. Sommacal, “The transition from regular to irregular motion as travel on Riemann surfaces”; *J. Phys. A: Math. Gen.* 38 (2005) 8873-8896.
- [9] F. Calogero and M. Sommacal, “Periodic solutions of a system of complex ODEs. II. Higher periods”, *J. Nonlin. Math. Phys.* **9** (2002), 483-516.
- [10] B. A. Dubrovin, A. T. Fomenko, and S. P. Novikov, *Modern Geometry-Methods and Applications: Part 1. The Geometry of Surfaces, Transformation Groups, and Fields*, volume 93 of Graduate Texts in Mathematics. Springer Verlag, 1992.

- [11] I. Dynnikov, S. Novikov, “Topology of Quasiperiodic Functions on the Plane”, *Uspekhi Math Nauk=Russian Math Surveys* (2005) v 60 n 1
- [12] Y. Fedorov and D. Gomez-Ullate, “Dynamical systems on infinitely sheeted Riemann surfaces”, arXiv:nlin.CD/0607028.
- [13] M. Kontsevich, Lyapunov exponents and Hodge theory. “The mathematical beauty of physics” (Saclay, 1996), (in Honor of C. Itzykson) 318–332, *Adv. Ser. Math. Phys.*, 24. World Sci. Publishing, River Edge, NJ (1997)
- [14] S. Kowalevski, “Sur le probleme de la rotation d’un corps solid autour d’un point fixé”, *Acta Math.*, **12**, 177-232 (1889). P. Painlevé, “Sur les équations differentielles du second ordre et d’ordre superieur dont l’integrale generale est uniforme”, *Acta Math.*, **25**, 1-85 (1902). B. Gambier, “Sur les equations differentielles du second ordre et du premier degre dont l’integrale generale est à points critiques fixes”, *Acta Math.*, **33**, 1-55 (1910).
- [15] E. Induti, “Sul moto nel piano complesso di particelle attratte verso l’origine con forze lineari ed interagenti a due corpi con forze proporzionali ad una potenza intera, negativa, dispari della loro distanza”; Tesi di Laurea, Università di Roma “La Sapienza”, Dipartimento di Fisica, Anno Accademico 2003-04. Advisor: Francesco Calogero.
- [16] A. Maltsev, S. Novikov. “Dynamical Systems, Topology and Conductivity in Normal Metals”. *Journal of the Statistical Physics*, **115**, No 1 April 2004, 31-46.
- [17] H. Masur, “Interval exchange transformations and measured foliations”. *Ann. of Math.*, **115**,(1982), 169-200.
- [18] S. P. Novikov, “The Hamiltonian Formalism and Many-Valued Analogs of the Morse Theory”, *Russian Math Surveys* **37**, No 5, (1982), 1-56.
- [19] S. P. Novikov, “Topology of the Generic Hamiltonian Foliations on the Riemann Surface”. arXiv: math.GT/0505342.
- [20] M. Tabor and J. Weiss, “Analytic structure of the Lorenz system”, *Phys. Rev. A* **24** 2157 (1981). A. Ramani, B. Grammaticos and T. Bountis, “The Painlevé property and singularity analysis of integrable and non-integrable systems”, *Physics Reports*, 160-163 (1989). T. Bountis, L.

- Drossos and I. Percival, “Non-integrable systems with algebraic singularities in complex time”, *J. Phys. A: Math. Gen.* **23**, 3217-3236 (1991). T. Bountis, “Investigating non-integrability and chaos in complex time”, *Physica D* **86**, 256-267 (1995). A. S. Fokas and T. Bountis, “Order and the ubiquitous occurrence of chaos”, *Physica A* **288**, 236-244 (1996). S. Abenda, V. Marinakis and T. Bountis, “On the connection between hyperelliptic separability and Painlevé integrability”, *J. Phys. A: Math. Gen.* **34**, 3521-3539 (2001).
- [21] F. Strocchi, “Complex Coordinates and Quantum Mechanics”, *Rev. Mod. Phys.* **38**, 36-40 (1966).
- [22] W. A. Veech. “Gauss measures for transformations on the space of interval exchange maps”. *Annals of Math.*, **115**, (1982), 201–242.
- [23] H. Yoshida, “Necessary condition for the existence of algebraic first integrals: I, II”, *Celes. Mech.* **31**, 363-379; 381-399 (1983). S. Ziglin, “Branching of solutions and nonexistence of first integrals in Hamiltonian mechanics; I, II”, *Func. Anal. Appl.* **16**, 181-189 (1983). S. Ziglin, “Self-intersection of the complex separatrices and the nonexistence of the integrals in the Hamiltonian systems with one-and-half degrees of freedom”, *J. Appl. Math.* **45**, 411-413 (1982). M. D. Kruskal and P. Clarkson, “The Painlevé-Kowalewski and poly-Painlevé tests for integrability”, *Studies Appl. Math.* **86**, (1992) 87-165. R. D. Costin and M. D. Kruskal, “Nonintegrability criteria for a class of differential equations with two regular singular points”, *Nonlinearity* **16**, 1295-1317 (2003). R. D. Costin, “Integrability properties of a generalized Lamé equation; applications to the Hénon-Heiles system, *Methods Appl. Anal.* **4**, 113-123 (1997).
- [24] A. Zorich, *Flat Surfaces*. “Frontiers in Number Theory, Physics and Geometry”, Proceedings of Les Houches winter school-2003, Springer Verlag 2006, 439-586.
- [25] A. Zorich, “Deviation for interval exchange transformations, *Ergodic Theory and Dynamical Systems*”, **17**, (1997), 1477-1499.
- [26] A. Zorich, “Asymptotic flag of an orientable measured foliation on a surface, in collection ”Geometric Study of Foliations”, World Scientific Pb. Co., (1994), 479-498.